TR-AC-0009

018

Smart MUSIC Algorithm

多賀　史江

1997. 9. 1

ATR環境適応通信研究所

Smart MUSIC algorithm

Fumie Taga

September 1, 1997

Contents

List of Figures

List of Tables

Abstract

Eigen-based methods have proven to be an effective means of obtaining Direction-Of-Arrival (DOA) estimates of multiple signals from outputs of sensor arrays. Among many algorithms, the MUltiple SIgnal Classification (MUSIC) algorithm is widely considered to be the most effective. However, MUSIC requires a considerable amount of computation because of the need for eigenvalue analysis of the covariance matrix and analysis of the MUSIC eigenspectrum. To reduce this computational load to the extent that the sensor array system may follow the rapid change of the radio environment, the author proposes the Smart MUSIC (S-MUSIC) algorithm. In S-MUSIC, the only requirements are the calculation of basis vectors in the space spanned by received data vectors without eigenvalue analysis, the calculation of only one vector orthogonal to the basis vectors, and a simpler MUSIC eigenspectrum than that of MUSIC. In this paper, S-MUSIC is introduced in detail and the superior characteristics of S-MUSIC's reduced processing time ($\frac{1}{100}$ to $\frac{1}{1000}$ that of MUSIC) and high resolution are shown by numerical simulation.

1 Introduction

Severe problems exist in the area of array processing involving the estimation of the Directions-Of-Arrival (DOA) of fully correlated signals. This case, referred to as the coherent signal case, appears in specular multipath propagation and is therefore of great practical importance. Unfortunately, the MUltiple SIgnal Classification (MUSIC) algorithm [1, 2], the minimum norm[3], and the minimum variance[4] fail in this case. A preprocessing technique that circumvents this difficulty, referred to as spatial smoothing, was introduced by Evans et al.[5] and Shan et al. [6], and further developed[7] - [16].

Rao et al.[11] analyzed effects of three preprocessing techniques. They labeled techniques presented by Schmidt[1, 2], Shan et al. [6], and Williams et al.[10] as the forward–only, the forward–only smoothing, and the forward–backward spatial smoothing techniques, respectively. Among them, the forward–backward spatial smoothing (FBSS) technique is considered to be the most effective, because FBSS can decorrelate the coherency best among these techniques. As a result, there are many applications [17, 18] of MUSIC with FBSS at present.

MUSIC with FBSS consists of three steps. The first step is to extract signal eigenvectors out of received data. The second step is to calculate noise eigenvectors. The third step is to form a MUSIC eigenspectrum by utilizing noise eigenvectors to estimate DOAs. Unfortunately, the computational load of MUSIC with FBSS is considerably large because of the need for eigenvalue analysis of the covariance matrix comprised of received data, and analysis of the MUSIC eigenspectrum (Ψ).

In analyzing Ψ, the range of directions under consideration is finely divided to ensure high resolution. This means that many directions have to be considered and noise eigenvectors have to be estimated through eigenvalue analysis. An algorithm for DOA estimation, which has the same high resolution as MUSIC but with a much smaller computational load, would be ideal for the sensor array system to follow the rapid change of the radio environment.

To reduce the computational load of MUSIC, the author first proposed an algorithm to estimate signal eigenvectors and noise eigenvectors with Gram-Schmidt orthogonalization in-

stead of eigenvalue analysis of the covariance matrix [19, 20, 21]. Then, she proposed a simplification of the Gram-Schmidt orthogonalization, called the Smart MUSIC algorithm (S-MUSIC)[22, 23].

In this paper, we introduce and explain S-MUSIC in detail. Then, we study characteristics of S-MUSIC, more specifically, its resolution limit and computational load, in comparison with identical characteristics of MUSIC.

First, the well-established MUSIC algorithm with FBSS is briefly reviewed. Then, the Smart MUSIC (S-MUSIC) algorithm is proposed. S-MUSIC does not have to utilize the covariance matrix of received data, and furthermore, it introduces a simpler Ψ than that in MUSIC, although S-MUSIC and MUSIC share the principle that direction/steering vectors corresponding to incident signals are orthogonal to noise eigenvectors. At the same time, the computational loads of S-MUSIC and MUSIC are roughly estimated. S-MUSIC is proven to impose a lower computational load than does MUSIC. Finally, it is demonstrated by numerical simulation that S-MUSIC has the same high resolution as MUSIC and that the computational load of S-MUSIC is $\frac{1}{100}$ to $\frac{1}{1000}$ that of MUSIC.

2 Problem Formulation

To simplify the numerical formula expression, the following notations are used in this paper.

$\boldsymbol{x}\ (i)$	the ith component of the vector $\boldsymbol{x}$
$\boldsymbol{X}\ (i,j)$	the component of the ith row and jth column of the matrix $\boldsymbol{X}$
$\dagger$	a Hermite conjugate
$\mathbf{E}\,[x]$	the expected value of x
$*$	a complex conjugate
$(\boldsymbol{x}, \boldsymbol{y})$	the inner product between a vector $\boldsymbol{x}^*$ and a vector $\boldsymbol{y}$.
$\mathbf{vct}\ {}_i^{\mathrm{MAX}}\ \lvert\boldsymbol{x}\rvert$	a vector $\boldsymbol{x}$ whose euclidean norm is at a maximum when the variable i is changed
$\mathbf{vl}\ {}_i^{\mathrm{MAX}}\ \lvert x\rvert$	a value x whose magnitude is at a maximum when the variable i is changed

Consider M linear equidistant omnidirectional sensors with a spacing of δ receiving P $(P < M)$ incident signals $S_p(t)(1 \leq p \leq P)$, with DOAs θ_p. They are embedded in stationary, ergodic Gaussian noise $\eta_m(t)(1 \leq m \leq M)$ with a zero mean and a covariance matrix $\sigma^2\ \boldsymbol{I}$, uncorrelated to impinging signals , where σ^2 is unknown and $\boldsymbol{I}$ is the identity matrix. We assume signals to be narrow-band with a central wavelength of λ. Received data $r_m(t)$ at each antenna is

$$r_m(t) = \sum_{p=1}^{P} \exp\left[\jmath \frac{2\pi}{\lambda} m\delta \sin\theta_p\right] S_p(t) + \eta_m(t). \tag{1}$$

Received data can be rewritten in matrix form as

$$\begin{aligned} \boldsymbol{r}(t) &= (\boldsymbol{d}_1 \cdots \boldsymbol{d}_P)\boldsymbol{S}(t) + \boldsymbol{\eta}(t) \\ &= \boldsymbol{D}\boldsymbol{S}(t) + \boldsymbol{\eta}(t), \end{aligned} \tag{2}$$

where

$$\boldsymbol{S}(t)(p) = S_p(t) \tag{3}$$

$$\boldsymbol{\eta}(t)(m) = \eta_m(t) \tag{4}$$

and $\boldsymbol{d}_p$ is the direction vector or the steering vector characterized by the sensor array as

$$\boldsymbol{D}(m,p)^1 = \boldsymbol{d}_p(m) = \exp\left[\jmath\frac{2\pi}{\lambda}m\delta\sin\theta_p\right]. \tag{5}$$

The covariance matrix of $\boldsymbol{r}(t)$ is

$$\mathbf{E}\left[\boldsymbol{r}(t)\boldsymbol{r}(t)^\dagger\right] = \boldsymbol{D}\mathbf{E}\left[\boldsymbol{S}(t)\boldsymbol{S}(t)^\dagger\right]\boldsymbol{D}^\dagger + \sigma^2\boldsymbol{I}, \tag{6}$$

where

$$\mathbf{E}\left[\boldsymbol{S}(t)\boldsymbol{S}(t)^\dagger\right](i,j) = \mathbf{E}\left[S_i(t)S_j(t)^*\right]. \tag{7}$$

When all incident signals are incoherent, which is the presupposition of MUSIC, the number of incident signals and their DOAs can be estimated by eigenvalue analysis of $\mathbf{E}\left[\boldsymbol{r}(t)\boldsymbol{r}(t)^\dagger\right]$. However, not all incident signals are incoherent. When some of incident signals are coherent, the matrix $\mathbf{E}\left[\boldsymbol{S}(t)\boldsymbol{S}(t)^\dagger\right]$ is singular and eigenvalue analysis of $\mathbf{E}\left[\boldsymbol{r}(t)\boldsymbol{r}(t)^\dagger\right]$ can not be correctly performed. Therefore, a preprocessing technique, where the decorrelation factor [24] $\sum_{k=1}^{K}\exp\left[\jmath\frac{2\pi}{\lambda}k\delta(\sin\theta_i - \sin\theta_j)\right]$ decorrelates $S_i(t)$ and $S_j(t)$ partially or completely, is applied to MUSIC because the nonsingularity of $\mathbf{E}\left[\boldsymbol{S}(t)\boldsymbol{S}(t)^\dagger\right]$ is a precondition to successfully applying the eigen-based method. This paper deals with the most problematic case, in which all incident signals are coherent.

3 MUSIC Algorithm with FBSS

This section reviews MUSIC with FBSS because it is presently considered to be the most effective means of estimating DOAs of coherent signals.

3.1 Estimation of Signal Eigenvectors and Noise Eigenvectors

An L-dimensional covariance submatrix $\boldsymbol{C}$ comprised of $\boldsymbol{r}(t)$ is formed, and its eigenvalue analysis is carried out. Consequently, P incident signals are counted and both P signal eigenvectors and $(L-P)$ noise eigenvectors are calculated.

3.1.1 Formation of the Covariance Submatrix

We define the measurement of the hth snapshot at time t_h to result in the M-dimensional vector of $\boldsymbol{r}(t_h)$. With the snapshot number of H, the covariance matrix of the received data is

$$\boldsymbol{R} = \frac{1}{H}\sum_{h=1}^{H}\boldsymbol{r}(t_h)\boldsymbol{r}(t_h)^\dagger. \tag{8}$$

The computational load at this stage is on the order of $M^2 H$. When all of incident signals are incoherent, $\boldsymbol{R}$ itself is utilized for the eigenvalue analysis in MUSIC. However, when some of incident signals are coherent, an L-dimensional smoothed covariance matrix $\boldsymbol{C}$

$$\begin{aligned} \boldsymbol{C}(i,j) &= \frac{1}{2K}\sum_{k=1}^{K}[\boldsymbol{R}(i+k-1, j+k-1)+ \\ &\quad \boldsymbol{R}(L+k-j, L+k-i)] \\ &\quad (1 \le i,j \le L < M; L+K-1=M) \end{aligned} \tag{9}$$

is utilized to estimate the signal and noise eigenvectors by FBSS. The computational load for the smoothing of covariance matrix $\boldsymbol{R}$ is on the order of $2K\ L^2$.

3.1.2 Eigenvalue Analysis

Eigenvalue analysis of $\boldsymbol{C}$ is performed with the result that the number of incident signals, signal eigenvectors, and noise eigenvectors are all estimated. Through eigenvalue analysis of $\boldsymbol{C}$, we get

$$\boldsymbol{C}\left[\boldsymbol{a}_1, \boldsymbol{a}_2, \cdots, \boldsymbol{a}_L\right] = \begin{pmatrix} \mu_1 & 0 & \cdots & 0 \\ 0 & \mu_2 & \cdots & 0 \\ \vdots & 0 & \ddots & \vdots \\ 0 & \cdots & \cdots & \mu_L \end{pmatrix} \left[\boldsymbol{a}_1, \boldsymbol{a}_2, \cdots, \boldsymbol{a}_L\right], \tag{10}$$

where μ_l $(1 \le l \le L)$ are eigenvalues, and $\boldsymbol{a}_l$ $(1 \le l \le L)$ are their corresponding eigenvectors of $\boldsymbol{C}$, which satisfy

$$\mu_L \le \cdots \le \mu_{P+1} \ll \mu_P \le \cdots \le \mu_1 \tag{11}$$

$$\boldsymbol{a}_L \perp \cdots \perp \boldsymbol{a}_{P+1} \perp \boldsymbol{a}_P \perp \cdots \perp \boldsymbol{a}_1, \tag{12}$$

when all incident signals are completely decorrelated. The eigenvectors $\boldsymbol{a}_l$ $(1 \le l \le P)$, corresponding to the lth largest eigenvalue, are signal eigenvectors and $\boldsymbol{a}_l$ $(P+1 \le l \le L)$, corresponding to the $(L-P)$ smaller eigenvalues, are noise eigenvectors.

MUSIC counts the number of P incident signals by finding μ_P satisfying $\mu_{P+1} \ll \mu_P$. The computational load of its eigenvalue analysis is approximately on the order of L^3.

3.2 MUSIC Eigenspectrum

In MUSIC, DOAs are estimated using the MUSIC eigenspectrum Ψ as

$$\Psi = \frac{1}{\sum_{l=P+1}^{L} |(\boldsymbol{d}_n, \boldsymbol{a}_l)|^2}, \qquad -\frac{\pi}{2} \le \theta_n \le \frac{\pi}{2}, \tag{13}$$

where $\boldsymbol{d}_n$ is defined as in Eq. (5) and successive θ_n are finely spaced to ensure high resolution. When θ_n is changed N times from $-\frac{\pi}{2}$ to $\frac{\pi}{2}$, the computational load of this stage is on the order of $NL(L-P)$.

3.3 Estimation with the miscounting of P

When MUSIC counts the number of incident signals P correctly, or when $\boldsymbol{a}_l$ $(1 \leq l \leq P)$ contain all signal constituents, DOAs can be perfectly estimated by Ψ in Eq. (13). In reality, however, the number of incident signals P is counted by finding μ_P satisfying $\frac{\mu_{P+1}}{\mu_1} \leq \mathcal{T}_h$, where $\mathcal{T}_h$ is appropriately set.

MUSIC was not proposed as a real-time signal processing algorithm, but as an algorithm to estimate the number and directions of incident signals without sticking to the processing time. Therefore, MUSIC carries out the calculation of Ψ with several values of $\mathcal{T}_h$ several times, util the estimation can be regarded as correct. However, there are no extra trials for the calculation with another $\mathcal{T}_h$ in the case of real-time signal processing.

Since the aim of this paper is to propose an algorithm applicable for real-time signal processing, we set an appropriate $\mathcal{T}_h$ beforehand to estimate DOAs even in the case of MUSIC and regard the results by this $\mathcal{T}_h$ as estimates of MUSIC. Here, without advance information on the noise and incident signals, the value of this $\mathcal{T}_h$ is not always ideal for the estimation of DOAs in MUSIC. Therefore, MUSIC does not always count all signals in all cases, but instead produces estimates less than the correct number of incident signals when $\mathbf{E}\left[\boldsymbol{S}(t)\boldsymbol{S}(t)^{\dagger}\right]$ is degenerate.

Therefore, it is worthwhile to discuss DOA estimation in cases MUSIC can not count the total number of incident signals. In estimation with the miscounting of P, $\boldsymbol{a}_l$ $(P+1 \leq l \leq L)$ contain some parts of signal constituents, and the DOA estimation by Ψ in Eq. (13) deteriorates. When the estimated number of incident signals differs from the assumed count, the estimated result is taken to mean MUSIC can not resolve the incident signals beyond the resolution limit.

4 Smart MUSIC Algorithm

In this section, the Smart MUSIC (S-MUSIC) algorithm is proposed. Furthermore, it is theoretically proven that the computational load of S-MUSIC is much smaller than that of MUSIC.

4.1 Estimation of Signal Eigenvectors and One Noise Eigenvector

MUSIC estimates signal eigenvectors and plural noise eigenvectors by implementing eigenvalue analysis of the covariance submatrix $\boldsymbol{C}$, comprised of received data $\boldsymbol{r}(t)$. S-MUSIC, in contrast, estimates signal eigenvectors and only one noise eigenvector without the eigenvalue analysis, and thus it requires less computations than MUSIC.

4.1.1 Signal Eigenvectors

S-MUSIC calculates basis vectors in the space spanned by

$$\mathbf{E}\left[\boldsymbol{r}_k\right] = \frac{1}{H}\sum_{h=1}^{H} \boldsymbol{r}_k(t_h), \tag{14}$$

where

$$\boldsymbol{r}_k(t_h) =$$

$$\begin{cases} [r_k(t_h), r_{k+1}(t_h), \cdots, r_{k+L-1}(t_h)]^{\mathrm{T}} \\ \qquad\qquad (1 \le k \le K) \\ [r_{M-k}(t_h)^*, r_{M-k-1}(t_h)^*, \cdots, r_{M-k-L+1}(t_h)^*]^{\mathrm{T}} \\ \qquad\qquad (K+1 \le k \le 2K) \end{cases} \tag{15}$$

and t_h satisfies the following equation with the light speed of v: $t_{h+1} - t_h = \dfrac{\lambda}{v}$. Here, the computational load to calculate $\mathbf{E}[\boldsymbol{r}_k]$ is in the order of $2KLH$. On the other hand, the computational load to calculate $\boldsymbol{C}$ in MUSIC is in the order of $M^2H + 2KL^2$.

Next, the computational load of basis vectors, which are regarded as signal eigenvectors in MUSIC, is estimated. To start, we first choose a starting basis vector $\boldsymbol{a}_1$ in the space spanned by $\mathbf{E}[\boldsymbol{r}_k]$ mapped by the equation

$$\boldsymbol{a}_1 = \mathbf{vct} \underset{1 \le k \le K}{\mathrm{MAX}} |\mathbf{E}[\boldsymbol{r}_k]|. \tag{16}$$

$\boldsymbol{a}_1$ is regarded as the eigenvector corresponding to the largest eigenvalue of $\boldsymbol{C}$ in MUSIC.

Then, $\mathbf{E}[\boldsymbol{r}_k]$ $(2 \le k \le 2K)$ are rearranged on the order of the magnitudes of $|(\mathbf{E}[\boldsymbol{r}_1], \mathbf{E}[\boldsymbol{r}_k])|$, $(2 \le k \le 2K)$ so that inequalities

$$\begin{aligned} |(\mathbf{E}[\boldsymbol{r}_1], \mathbf{E}[\boldsymbol{r}_2])| &\le |(\mathbf{E}[\boldsymbol{r}_1], \mathbf{E}[\boldsymbol{r}_3])| \\ &\le \cdots \le |(\mathbf{E}[\boldsymbol{r}_1], \mathbf{E}[\boldsymbol{r}_{2K}])| \end{aligned} \tag{17}$$

are satisfied.

Then, the other basis vectors $\boldsymbol{a}_k$ $(2 \le k \le P)$ in the space spanned by $\mathbf{E}[\boldsymbol{r}_k]$ are calculated through the iteration of the equation:

$$\boldsymbol{a}_k = \mathbf{E}[\boldsymbol{r}_k] - \sum_{\kappa=1}^{k-1} \frac{(\boldsymbol{a}_\kappa, \mathbf{E}[\boldsymbol{r}_k])}{|\boldsymbol{a}_\kappa|} \frac{\boldsymbol{a}_\kappa}{|\boldsymbol{a}_\kappa|} \quad (2 \le k \le P). \tag{18}$$

P incident signals are counted by finding the value $|\boldsymbol{a}_{P+1}|$, which is assumed as 0.

The computational load of basis vectors $\boldsymbol{a}_k$ $(1 \le k \le P)$ is on the order of $2KL$ when $P = 1$, and $4KL - 2L + \sum_{k=2}^{P} L(3k-2)$ when $P \ge 2$.

4.1.2 One Noise Eigenvector

In MUSIC, $L - P$ noise eigenvectors are calculated by eigenvalue analysis. When DOA estimation is based on the idea that the direction vectors of incident signals are orthogonal to noise eigenvectors, just one noise eigenvector is theoretically sufficient to estimate the DOAs. FKMUSIC in [20] calculates several noise eigenvectors which is less than $(L - P)$ in number. However, the number of noise eigenvectors and the way unit vectors are established for these noise eigenvectors remain unresolved issues.

To resolve these issues, we propose an approach that calculates only one effective noise eigenvector for DOA estimation. Furthermore, we prove that the computational load for both signal eigenvectors and one noise eigenvector in S-MUSIC is much smaller than that for the formation of $\boldsymbol{C}$ and its eigenvalue analysis in MUSIC.

In S-MUSIC, we first find the number $\mathcal{L}$ which is the number of one of components of $\boldsymbol{a}_1$, and $|\boldsymbol{a}_1(\mathcal{L})|$ has the maximum value among $|\boldsymbol{a}_1(l)|$ $(1 \leq l \leq L)$. Then, $\mathcal{L}$ satisfies

$$\boldsymbol{a}_1(\mathcal{L}) = \mathrm{vl}\ \overset{\mathrm{MAX}}{1 \leq l \leq L}\ |\boldsymbol{a}_1(l)|. \tag{19}$$

Next, we set up the unit vector $\boldsymbol{u}$ as

$$\boldsymbol{u} \triangleq \left[\overset{1}{0}\ 0\ 0\ \overset{\mathcal{L}}{1}\ 0\ 0\ 0\ \overset{L}{0}\right]^{\mathrm{T}}, \tag{20}$$

in which all of the elements except the $\mathcal{L}$th value are 0. Then, after all $\boldsymbol{a}_k$ $(1 \leq k \leq P)$ have been calculated, one noise eigenvector $\boldsymbol{a}_{\mathcal{N}}$ is estimated by the equation

$$\boldsymbol{a}_{\mathcal{N}} = \boldsymbol{u} - \sum_{k=1}^{P} \frac{(\boldsymbol{a}_k{}^*, \boldsymbol{u})}{|\boldsymbol{a}_k|} \frac{\boldsymbol{a}_k}{|\boldsymbol{a}_k|}. \tag{21}$$

The computational load for $\boldsymbol{a}_{\mathcal{N}}$ is on the order of $3LP$.

4.2 MUSIC Eigenspectrum

We propose a simple MUSIC eigenspectrum Ψ and estimate the computational load. In MUSIC, $L - P$ noise eigenvectors are utilized for Ψ in Eq. (13). However, in S-MUSIC, only one noise eigenvector is utilized. DOAs are estimated using Ψ as

$$\Psi = \frac{1}{|(\boldsymbol{d}_n, \boldsymbol{a}_{\mathcal{N}})|^2}, \qquad -\frac{\pi}{2} \leq \theta_n \leq \frac{\pi}{2}. \tag{22}$$

Therefore, the computational load for Ψ in Eq. (22) is on the order of NL, while that of MUSIC is on the order $NL(L - P)$.

4.3 Comparison of computational loads

Here, we summarize both S-MUSIC and MUSIC and at the same time, estiamte the computational load at each step.

MUSIC	S-MUSIC
(1)Covariance matrix $\boldsymbol{R}$ of received data $\boldsymbol{r}(t_h)$ in Eq. (8)$[M^2H]$ (2) Smoothed covariance submatrix $\boldsymbol{C}$ in Eq. (9)$[2KL^2]$	(a) Ensemble mean of received data $\boldsymbol{r}(t_h)$ in Eq. (14)$[2KLH]$
(3)Eigenvalue analysis of $\boldsymbol{C}$ in Eq. (25)$[L^3]$	(b) Detection of the largest vector in Eq. (16) $[2LK]$ (c)Rearrangement of $\mathbf{E}[\boldsymbol{r}_k]$ in Eq. (17) $[2L(2K-1)]$ (d) Basis vectors $\boldsymbol{a}_k$ in Eq. (18) $\left[\sum_{k=2}^{P}\{3L(k-1)+L\}\right]$ (e) Detection of $\mathcal{L}$ in Eq. (19) $[2L]$ (f) Noise eigenvector $\boldsymbol{a}_{\mathcal{N}}$ in Eq. (21) $[L(3P-2)]$
(4)MUSIC Eigenspectrum in Eq. (13) $[NL(L-P)]$	(g)MUSIC Eigenspectrum in Eq. (22) $[NL]$

When we set the value of L appropriately, that is, as $\frac{4}{5}M$, the value of K $(= M - L + 1)$ becomes $\frac{L}{4} + 1$. Furthermore, when we set the value of P as $\frac{2L}{5}$, the computational loads of S-MUSIC and MUSIC are on the order of $\frac{6L^3}{25} + (\frac{H}{2} + 2)L^2 + (2H + N + 1)L$ and $\frac{3L^3}{2} + (\frac{25H}{16} + \frac{3N}{5} + 2)L^2$, respectively. Even if we pay attention only to the term L^3, the rate of increase of the computational load to L in MUSIC is more than 6 times that in S-MUSIC.

4.4 Estimation with the miscounting of P

This subsection discusses DOA estimation in the case S-MUSIC can not count the number of incident signals and shows a way to estimate the number of incident signals S-MUSIC counts. When the number of incident signals P has correctly been counted, or when $\boldsymbol{a}_k$ $(1 \leq k \leq P)$ contain all signal constituents, DOAs can be completely estimated by Ψ in Eq. (22). In reality, however, the iteration in Eq. (18) is stopped, and the number of incident signals P is determined when a value $|\boldsymbol{a}_{P+1}|$ is found that satisfies $\frac{|\boldsymbol{a}_{P+1}|}{|\boldsymbol{a}_1|} \leq \mathcal{T}_h$. When only $\mathcal{P}$ $\boldsymbol{a}_k$ $(1 \leq k \leq \mathcal{P} < P)$ are calculated in Eq. (18) and utilized in Eq. (21), the orthogonality between $\boldsymbol{a}_{\mathcal{N}}$ and $\boldsymbol{a}_k$ $(1 \leq k \leq P)$ is

$$\left|\left(\frac{\boldsymbol{a}_k}{|\boldsymbol{a}_k|}, \frac{\boldsymbol{a}_{\mathcal{N}}}{|\boldsymbol{a}_{\mathcal{N}}|}\right)\right| =$$

$$\begin{cases} 0 & \\ & (1 \le k \le \mathcal{P}) \\ \left|\left(\dfrac{\boldsymbol{a}_k}{|\boldsymbol{a}_k|}, \dfrac{\boldsymbol{u}}{|\boldsymbol{a}_\mathcal{N}|}\right)\right| = \dfrac{|\boldsymbol{a}_k(\mathcal{L})^*|}{|\boldsymbol{a}_k||\boldsymbol{a}_\mathcal{N}|}, & \\ & (\mathcal{P}+1 \le k \le P) \end{cases} \tag{23}$$

where $|\boldsymbol{a}_\mathcal{N}|$ is independent of k.

When $\boldsymbol{a}_k$ $(\mathcal{P}+1 \le k \le \mathcal{Q})$ include the signal component, $\dfrac{|\boldsymbol{a}_k(\mathcal{L})^*|}{|\boldsymbol{a}_k||\boldsymbol{a}_\mathcal{N}|}$ or $\dfrac{|\boldsymbol{a}_k(\mathcal{L})^*|}{|\boldsymbol{a}_k|}$ $(\mathcal{P}+1 \le k \le \mathcal{Q})$ in Eq. (23) becomes nearly 0. In this case, the noise eigenvector $\boldsymbol{a}_\mathcal{N}$ is orthogonal to $\boldsymbol{a}_k$ $(1 \le k \le \mathcal{Q})$. This means that in S-MUSIC, $\mathcal{Q}$ DOAs can be estimated by $\boldsymbol{a}_\mathcal{N}$, although $\boldsymbol{a}_\mathcal{N}$ is calculated with only $\mathcal{P}$ $\boldsymbol{a}_k$ $(1 \le k \le \mathcal{P} \le \mathcal{Q})$. Therefore, we can estimate the number of incident signals $\mathcal{Q}$ by analyzing $\dfrac{|\boldsymbol{a}_k(\mathcal{L})^*|}{|\boldsymbol{a}_k|}$ $(\mathcal{P}+1 \le k \le 2K)$. When $P \le \mathcal{Q}$, S-MUSIC can resolve all incident signals.

5 Numerical Simulation

We examine the computational load of S-MUSIC while varying M, in comparison with MUSIC. Furthermore, after defining the resolution limit, we examine this resolution limit with a variety of $\mathcal{T}_h$ and SNR values.

5.1 Processing Time

The computational load was roughly estimated in the previous sections. However, the estimation of the computational load in eigenvalue analysis remains in obscurity because we utilize a computational library for calculation in eigenvalue analysis on a workstation. Therefore, we measure the processing time of S-MUSIC or MUSIC to study how this processing time is affected by M. The workstation we utilize for the numerical simulation is a DEC alpha 3000/900.

P has a great effect on the resolution limit and, thus, on the estimation of $\mathcal{P}$. When P is large, the change of $\mathcal{P}$ has an effect on the processing time of S-MUSIC.

First, to restrain the effect of $\mathcal{P}$ and examine the effect of M, we set the number of incident signals P as a smallish number, i.e., 2.

Figure 1 shows the processing time of S-MUSIC and MUSIC when there are two $(P = 2)$ incident signals without additive noise. The number of antenna elements M ranged from 30 to 1000, $L = 0.8M$, $\mathcal{T}_h$ was set as 0.5 for S-MUSIC and 10^{-3} for MUSIC, and N was set as 20.

Lines (A) and (B) give the processing time of S-MUSIC and MUSIC, respectively.

The gradient of line (B) in the case of MUSIC is about twice that of line (A) in the case of S-MUSIC. This means that the effect of M on the processing time of MUSIC was bigger than that of S-MUSIC. In other words, the processing time of MUSIC was largely accounted for by eigenvalue analysis of covariance submatrix $\boldsymbol{C}$, compared with the analysis of Ψ. The processing time of S-MUSIC was $\dfrac{1}{100}$ to $\dfrac{1}{1000}$ that of MUSIC.

Next, we changed P, so that the ratio of $\frac{P}{M}$ could be constant with varing M. The lines from (a) to (f) in Figure 2 are the processing times of S-MUSIC when $\frac{P}{M}$ is $\frac{2i}{25}$ $(i = 1 \sim 7)$. The line (g) is the processing time of MUSIC. $\frac{P}{M}$ does not have a great effect on the processing time of MUSIC. The processing times of S-MUSIC are $\frac{1}{6}$ $(\frac{P}{M} = \frac{14}{25})$ to $\frac{1}{60}$ $(\frac{P}{M} = \frac{4}{25})$ that of MUSIC. Consequently, the smaller $\frac{P}{M}$ is, the shorter the processing time of S-MUSIC is, compared with that of MUSIC.

5.2 Resolution Limit

We examine the resolution limits of S-MUSIC and MUSIC and ascertain that these resolution limits are of the same order.

5.2.1 Definition of resolution limit

Figure 3 is an example of DOA estimation by MUSIC when there are three ($P = 3$) incident signals set at intervals of $\Delta\theta$ (0deg. $\leq \Delta\theta \leq$ 10deg.) with additive noise of 0dB. The array system has 32 ($M = 32$) antenna elements. L and K are set as 25 and eight, respectively. $\mathcal{T}_h$ is set as 10^{-3} and the snapshot number H is set to 70.

Area (a) is the range of 25 % fluctuation from the given DOAs. Area (b) is a range containing all of the estimated DOAs of area (a). Area (b) consists of two parts; 5.75deg. $\leq \Delta\theta \leq$ 6.2deg. and 7.4deg. $\leq \Delta\theta$. In this case, the resolution limit is designated as 7.4deg., not 5.75deg.

Simulations of this type are carried out several times. In this paper, the number of Monte Carlo runs is set as 30. When all DOAs are estimated with a $\Delta\theta$ in 85 % of the Monte Carlo runs, this $\Delta\theta$ is regarded to be within the resolution limit.

5.2.2 Influence of threshold $\mathcal{T}_h$

The resolution limit is changed by the threshold $\mathcal{T}_h$. Figure 4 shows the resolution limit of MUSIC, with $\mathcal{T}_h$ varying from 10^{-4} to 0.7. H and P are set as 70 and 3, respectively. When $\mathcal{T}_h$ is under some value, the resolution limit becomes stable. This $\mathcal{T}_h$ depends on P and SNR. Note that P and SNR do not have a great influence on the tendency for the resolution limit to be better with a smaller $\mathcal{T}_h$. In this paper, based on the stable range in Figure 4, $\mathcal{T}_h$ in MUSIC is fixed as 10^{-3}.

On the other hand, the resolution limit of S-MUSIC does not change greatly with varying $\mathcal{T}_h$ and P. This means that S-MUSIC can estimate DOAs correctly with $\Delta\theta$,which is within the resolution limit, even when the number of calculated signal eigenvectors is under P. As a result, S-MUSIC can decrease the computational load by setting $\mathcal{T}_h$ as a relatively large value. In this paper, $\mathcal{T}_h$ in S-MUSIC is fixed as 0.5.

5.2.3 Influence of snapshot number H

Figure 5 shows the resolution limits obtained when $\mathcal{T}_h$ in S-MUSIC, and $\mathcal{T}_h$ in MUSIC are set as 0.5 and 10^{-3}, respectively, and H ranges from 10 to 70. $\frac{P}{M}$, M, and SNR are $\frac{4}{25}$, 100,

and 0dB, respectively. The extent of the change in the resolution limit in S-MUSIC is smaller than that in MUSIC. The smaller H is, the lower the computational load is. Therefore, when H is set as a small value to decrease the computational load, the resolution limit of S-MUSIC is better than that of MUSIC. In this paper, however, H is fixed as 70.

5.2.4 Influence of the number of antennas M

Figure 6 shows the resolution limits of S-MUSIC and MUSIC when SNR and $\frac{P}{M}$ are fixed and M ranges from 25 to 250. Lines (a), (b), and (c) are the resolution limits of S-MUSIC and lines (d), (e), and (f) are those of MUSIC. The values of SNR and $\frac{P}{M}$ for each case are as follows:

line	(a), (d)	(b), (e)	(c), (f)
SNR	5dB	15dB	15dB
$\frac{P}{M}$	$\frac{4}{25}$	$\frac{4}{25}$	$\frac{12}{25}$

In S-MUSIC and MUSIC, as M becomes larger and $\frac{P}{M}$ becomes smaller, the resolution limit becomes better. When SNR and $\frac{P}{M}$ are relatively higher, the resolution limit of S-MUSIC is better than that of MUSIC.

5.2.5 Influence of the ratio $\frac{P}{M}$

Figure 7 shows the resolution limits obtained when M and SNR are fixed and $\frac{P}{M}$ ranges from $\frac{4}{25}$ to $\frac{14}{25}$. Lines (a), (b), and (c) are the resolution limits of S-MUSIC and lines (d), (e), and (f) are those of MUSIC. The values of M and SNR for each case are as follows:

line	(a), (d)	(b), (e)	(c), (f)
M	25	25	150
SNR	10dB	15dB	15dB

In every case, the resolution limit of S-MUSIC is better than that of MUSIC. Furthermore, when $\frac{P}{M}$ becomes higher, the difference between the resolution limit of S-MUSIC and that of MUSIC becomes larger. As a result, the resolution limit of S-MUSIC is much better than that of MUSIC when $\frac{P}{M}$ becomes larger.

5.2.6 Influence of additive noise

Figure 8 is the resolution limit when M and $\frac{P}{M}$ are fixed and SNR ranges from 0dB to 20dB. Lines (a), (b), and (c) are the resolution limits of S-MUSIC and lines (d), (e), and (f) are those of MUSIC. The values of M and $\frac{P}{M}$ for each case are as follows:

line	(a), (d)	(b), (e)	(c), (f)
M	25	125	25
$\frac{P}{M}$	$\frac{4}{25}$	$\frac{4}{25}$	$\frac{6}{25}$

The resolution limits of S-MUSIC and MUSIC are almost of the same order. However, for both (a) and (d) with an SNR larger than 5dB, and for both (c) and (f) with an SNR larger than 10dB, the resolution limit of S-MUSIC is better than that of MUSIC.

The reason why the resolution limit of S-MUSIC is worse than that of MUSIC with a lower SNR is as follows: The aim of Eq. (19) is to find the position of the element where the induced electricity by incident signals is the highest in $\boldsymbol{a}_1$, which consists of received raw data. As the SNR decreases, however, the noise has a larger effect on the received data and as a result, we fail to find the desired position in Eq. (19). In this case, $\boldsymbol{a}_N$ in Eq. (21), which is obtained from Eq. (20), is not the most desirable. Therefore, the resolution limit becomes worse.

6 Conclusion

This paper proposed the Smart MUSIC algorithm (S-MUSIC). Furthermore, the paper presented a study on the characteristics of S-MUSIC, in comparison with the same characteristics in the MUSIC algorithm (MUSIC).

In MUSIC, the computational load of eigenvalue analysis on the covariance matrix of received data and the analysis of the MUSIC eigenspectrum is considerably large.

S-MUSIC, in contrast, calculates only a few basis vectors in the space spanned by received data vectors and only one vector orthogonal to basis vectors without eigenvalue analysis of the covariance matrix, to reduce the computational load to the extent that the sensor array system may follow the rapid change of the radio environment. Here, basis vectors correspond to signal eigenvectors and the one orthogonal vector corresponds to noise eigenvectors in MUSIC. Furthermore, in the MUSIC eigenspectrum, S-MUSIC uses only one noise eigenvector. As a result, the computational load of MUSIC has been reduced significantly $\left(\frac{1}{100} \text{ to } \frac{1}{1000}\right)$ when P is fixed.

Numerical simulations have shown that S-MUSIC can decrease the computational load by setting $\mathcal{T}_h$ as a relatively large value, without deterioration of the resolution limit; the resolution limit of S-MUSIC is better than that of MUSIC, when H is set as a small value to decrease the computational load and both SNR and $\frac{P}{M}$ are set relatively higher. In the numerical simulations, the superiority of S-MUSIC over MUSIC was shown by the obtained small computational load, and it was ocnfirmed that S-MUSIC had the same high resolution as MUSIC.

7 What we should do afterwards

Estimation of signal parameters via rotational invariance techniques (the ESPRIT algorithm)[25, 26] was proposed to overcome one of the disadvantages in MUSIC. The disadvantage is that the information about the array sensors must be known a priori. However, the advantages in the ESPRIT algorithm were not only the decrease of the a priori information requirement by using two identical arrays of sensors, but also the reduction of the computational load in MUSIC. Nowadays, there are several papers [27, 28] which utilize the ESPRIT algorithm as the algorithm with smaller computational load than MUSIC. Therefore, the comparison between the ESPRIT algorithm and S-MUSIC is informative. Here, the ESPRIT algorithm is briefly introduced.

The ESPRIT Algorithm requires two subarrays of sensors that are identical but separated by a known displacement vector $\boldsymbol{\zeta}$. The outputs of the subarrays are modeled as the L

dimensional vectors $\boldsymbol{r}_1(t)$ and $\boldsymbol{r}_2(t)$. In this model, the received data $\boldsymbol{r}(t)$ is

$$\boldsymbol{r}(t) = \begin{bmatrix} \boldsymbol{r}_1(t) \\ \boldsymbol{r}_2(t) \end{bmatrix}, \tag{24}$$

which is the $2L$ dimensional vector. The covariance matrix of $\boldsymbol{r}(t)$ is the $2L \times 2L$ matrix $\mathbf{E}\left[\boldsymbol{r}(t)\boldsymbol{r}(t)^\dagger\right]$.

Through eigenvalue analysis of $\mathbf{E}\left[\boldsymbol{r}(t)\boldsymbol{r}(t)^\dagger\right]$, we get

$$\mathbf{E}\left[\boldsymbol{r}(t)\boldsymbol{r}(t)^\dagger\right][\boldsymbol{a}_1, \boldsymbol{a}_2, \cdots, \boldsymbol{a}_{2L}] = \begin{pmatrix} \mu_1 & 0 & \cdots & 0 \\ 0 & \mu_2 & \cdots & 0 \\ \vdots & 0 & \ddots & \vdots \\ 0 & \cdots & \cdots & \mu_{2L} \end{pmatrix} [\boldsymbol{a}_1, \boldsymbol{a}_2, \cdots, \boldsymbol{a}_{2L}], \tag{25}$$

where μ_l $(1 \leq l \leq 2L)$ are eigenvalues, and $\boldsymbol{a}_l$ $(1 \leq l \leq 2L)$ are their corresponding eigenvectors of $\mathbf{E}\left[\boldsymbol{r}(t)\boldsymbol{r}(t)^\dagger\right]$, which satisfy

$$\mu_{2L} \leq \cdots \leq \mu_{P+1} \ll \mu_P \leq \cdots \leq \mu_1 \tag{26}$$

$$\boldsymbol{a}_{2L} \perp \cdots \perp \boldsymbol{a}_{P+1} \perp \boldsymbol{a}_P \perp \cdots \perp \boldsymbol{a}_1. \tag{27}$$

Here, the $2L \times P$ matrix $[\boldsymbol{a}_1, \boldsymbol{a}_2, \cdots, \boldsymbol{a}_P]$ can be divided into two $L \times P$ matrices, $\mathcal{F}_1$ and $\mathcal{F}_2$ as follows:

$$[\boldsymbol{a}_1, \boldsymbol{a}_2, \cdots, \boldsymbol{a}_P] = \begin{bmatrix} \mathcal{F}_1 \\ \mathcal{F}_2 \end{bmatrix}. \tag{28}$$

Through eigenvalue analysis of the $2P \times 2P$ matrix $\begin{bmatrix} \mathcal{F}_1^\dagger \\ \mathcal{F}_2^\dagger \end{bmatrix} [\mathcal{F}_1 \mathcal{F}_2]$, we get the $2P$ dimensional eigenvectors $\boldsymbol{b}_p$ $(1 \leq p \leq 2P)$. The $2P \times 2P$ matrix $[\boldsymbol{b}_1, \boldsymbol{b}_2, \cdots, \boldsymbol{b}_{2P}]$ can be divided into 4 $P \times P$ matrices $\mathcal{B}_{11}$, $\mathcal{B}_{12}$, $\mathcal{B}_{21}$, and $\mathcal{B}_{22}$ as follows:

$$[\boldsymbol{b}_1, \boldsymbol{b}_2, \cdots, \boldsymbol{b}_{2P}] = \begin{bmatrix} \mathcal{B}_{11} & \mathcal{B}_{12} \\ \mathcal{B}_{21} & \mathcal{B}_{22} \end{bmatrix} \tag{29}$$

Through eigenvalue analysis of the $P \times P$ matrix $-\mathcal{B}_{12}\,\mathcal{B}_{22}^{-1}$, we get P eigenvalues φ_p $(1 \leq p \leq P)$. These eigenvalues satisfy the equation

$$\sin\theta_p = \frac{\lambda\varphi_p}{2\pi\zeta}. \tag{30}$$

Therefore, in the ESPRIT algorithm, θ_p can be estimated without the calculation of the MUSIC eigenspectrum.

Acknowledgments

The author gratefully acknowledges useful discussions with Dr. Yoshio Karasawa and Dr. Abdesselam Klouche-Djedid and would also like to thank Dr. Bokuji Komiyama and Dr. Eiichi Ogawa for their constructive comments that helped the author achieve her aims.

References

[1] R. O. Schmidt, "Multiple emitter location and signal parameter estimation," *Proc. RADC Spectral Est. Workshop,* pp. 243–258, 1979.

[2] R. O. Schmidt, "A signal subspace approach to multiple source location and spectral estimation," *Ph. D dissertation,* Stanford Univ., Stanford, CA, 1981.

[3] R. Kumaresan and D. W. Tufts, "Estimating the angle of arrival of multiple plain waves," *IEEE Trans. Aerosp. Electron. Syst.,* vol. AES-19, pp. 134–139, 1983.

[4] J. Capon, "High resolution frequency wave number spectrum analysis," *Proc. IEEE,* vol. 57, pp. 1408–1418, 1968.

[5] J. E. Evans, J. R. Johnson D. F. Sun, "Application of advanced signal processing techniques to angle of arrival estimation in ATC navigation and surveillance systems," *M. I. T. Lincoln Lab.,* Lexington, MA, Tech, Rep, 582, June 1982.

[6] T.J. Shan, M. Wax, T. Kailath, "On spatial smoothing for direction-of-arrival estimation of coherent signals," *IEEE Trans. Acoust., Speech, Signal Processing,* vol. ASSP-33, pp. 806–811, Aug. 1985.

[7] W. F. Gabriel, "Adaptive superresolution of coherent RF spatial sources," *Proc. 1st ASSP Workshop Spectral Estimation,* Hamilton, Ont., Canada, pp. 134–139, 1981.

[8] B. Widrow, K. M. Duvall, R. P. Gooch, W. C. Newman, "Signal cancelation phenomena in adaptive antennas: Causes and cures," *IEEE Trans. Antennas & Propag.,* vol. AP-30, pp. 469–478, 1982.

[9] H. Wang, M. Kaveh, "Coherent signal-subspace processing for detection and estimation of angles of arrival of multiple wide-band sources," *IEEE Trans. Acoust., Speech, Signal Processing,* vol. ASSP-33, pp. 823–831, Aug. 1985.

[10] R. T. Williams, S. Prasad, A. K. Mahalanabis, L. H. Sibul, "An improved spatial smoothing technique for bearing estimation in a multipath environment," *IEEE Trans. Acoust., Speech, Signal Processing,* vol. ASSP-36, pp. 425–431, Apr. 1988.

[11] B. D. Rao, K. V. S. Hari, "Effect of spatial smoothing on the performance of MUSIC and the minimum-norm method," *IEE Proc., ,* vol. 137, Pt. F, pp. 449–458, Dec. 1990.

[12] W. Du, R. L. Kirlin, "Improved spatial smoothing technique for DOA estimation of coherent signals," *IEEE Trans. Signal Processing,* vol. 39, pp. 1208–1210, May. 1991.

[13] R. D. DeGroat, E. M. Dowling, D. A. Linebarger, "The constrained MUSIC problem," *IEEE Trans. Signal Processing,* vol. 41, pp. 1445–1449, Mar. 1993.

[14] F. Taga, H. Shimotahira, K. Iizuka, "An approach to an ultra resolution fault locator," *Proc. Int. Laser Radar Conf.,* pp. 237–239, Jul. 1994.

[15] F. Taga, H. Shimotahira, "An Improved MUSIC Algorithm for High Resolution Image Reconstruction," *Proc. AP-S,* pp. 1342–1345, Jun. 1995.

[16] F. Taga, H. Shimotahira, "A Novel Spatial Smoothing Technique for the MUSIC Algorithm," *IEICE Trans. Commun.,* vol. E78-B, pp. 1513–1517, Nov. 1995.

[17] M. Wax, J, Sheinvald, "Direction finding of coherent signals via spatial smoothing for uniform circular arrays," *IEEE Trans. Antennas & Propag.,* vol. AP-42, pp. 613–620, May. 1994.

[18] J. W. Odendaal, E. Barnard, C. W. I. Pistorius, "Two-dimensional superresolution radar imaging using the MUSIC algorithm," *IEEE Trans. Antennas & Propag.,* vol. AP-42, pp. 1386–1391, Oct. 1994.

[19] H. Shimotahira, F. Taga, "On the Kernel MUSIC Algorithm with a Non-redundant Spatial Smoothing Technique," *IEICE Trans. Fundamentals ,* vol. E79-A, pp.1225–1231, Aug. 1996

[20] F. Taga, H. Shimotahira, "Proposal of the Fast Kernel MUSIC Algorithm, " *IEICE Trans. Fundamentals ,* vol. E79-A, pp. 1232-1239, Aug. 1996

[21] F. Taga, H. Shimotahira, "FAST KERNEL MUSIC ALGORITHM, " *Proc.IEEE GLOBECOM'96 ,* pp. 2028–2033, Nov. 1996

[22] F. Taga, "Smart MUSIC Algorithm for DOA estimation, " *IEE Electronics Letters,* vol. 33, No. 3, pp. 190–191, Jan. 1997.

[23] F. Taga, " The Smart MUSIC Algorithm, " *IEICE Gene. Conf.,* pp. 689–690, Mar. 1997.

[24] F. Taga, K. Takao, "Spatial Smoothing Technique Applied to Two-Dimensional Adaptive Arrays to Suppress Coherent Interferences, " *IEICE Tech. Rep. ,* A·P91-20, pp. 99–106, May, 1991.

[25] A. Paulraj, R. Roy, T. Kailath, "A subspace rotation approach to signal parameter estimation, " *Proc. IEEE ,* Vol.74, no. 7, pp. 1044–1045, July, 1986.

[26] R. Roy, T. Kailath, "ESPRIT–Estimation of signal parameters via rotational invariance techniques, " *IEEE Trans. Acoust., Speech, Signal Processing,* Vol.37, no. 7, pp. 984–995, July, 1989.

[27] Jerome A. Gansman, Michael D. Zoltowski, "Multidimensional Multirate DOA Estimation in Beamspace, " *IEEE Trans. Signal Processing,* Vol.44, no. 11, pp. 2780–2792, Nov., 1996.

[28] Norman Yuen, Benjamin Friedlander, "Asymptotic Performance Analysis of ESPRIT, Higher Order ESPRIT, and Virtual ESPRIT Algorithms, " *IEEE Trans. Signal Processing,* Vol.44, no. 10, pp. 2573–2550, Oct., 1996.

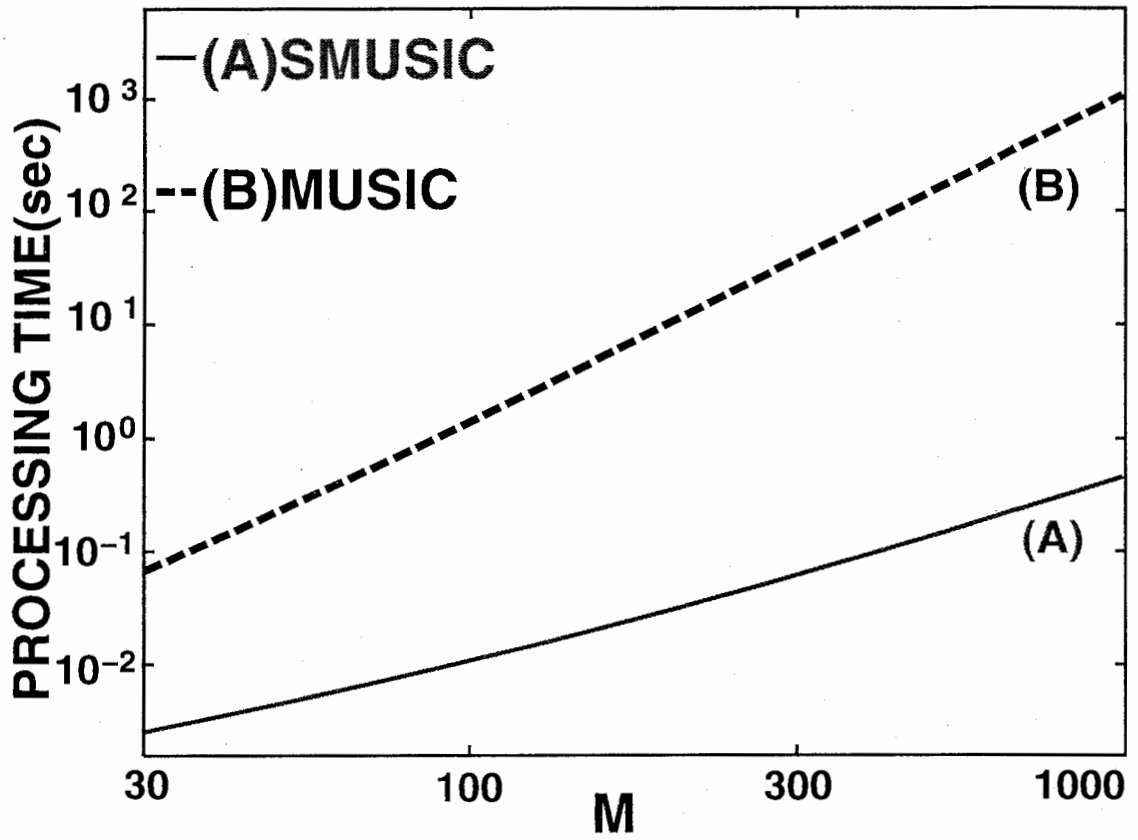

Figure 1: Processing times of SMUSIC and MUSIC when there are two ($P = 2$) incident signals without additive noise. The number of antenna elements M ranged from 30 to 1000, $L = 0.8M$, $\mathcal{T}_h$ was set as 0.5 for SMUSIC and 10^{-3} for MUSIC, and N was set as 20. Lines (A) and (B) are the processing times of S-MUSIC and MUSIC, respectively.

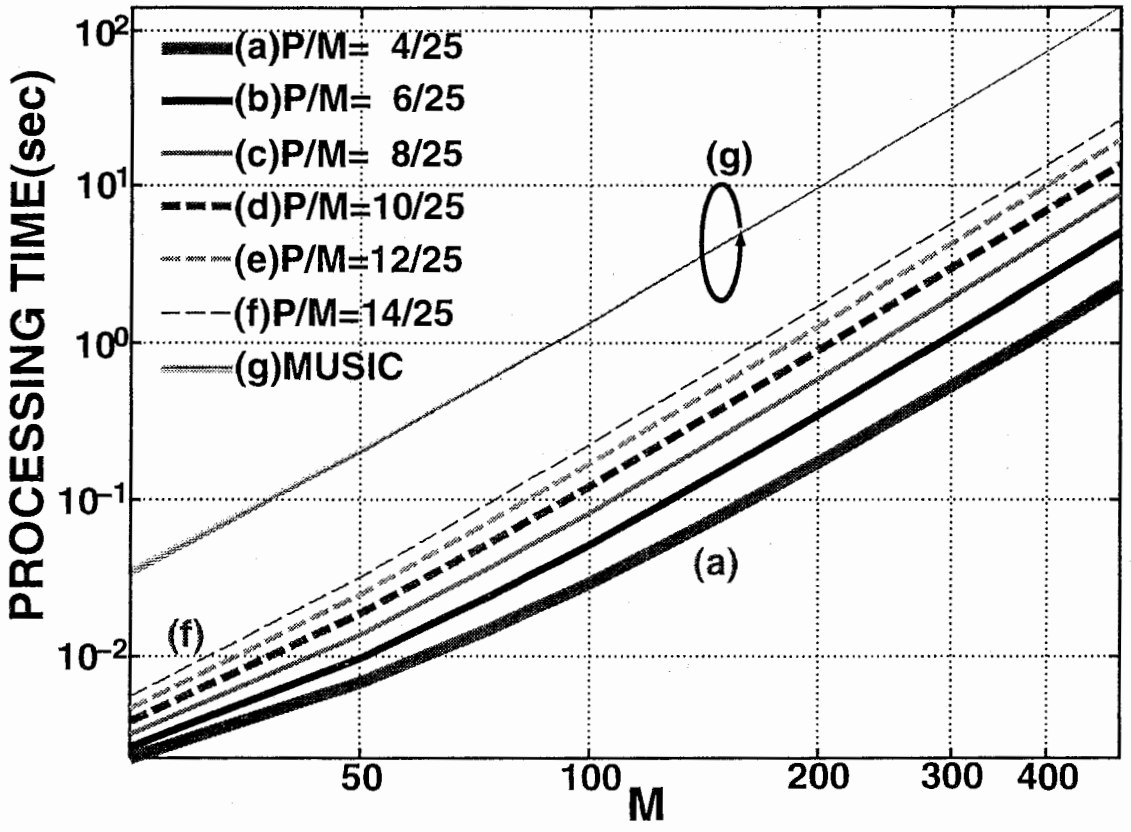

Figure 2: Processing times of S-MUSIC when $\frac{P}{M}$ is $\frac{2i}{25}$ $(i = 1 \sim 7)$. Line (g) is the processing time of MUSIC.

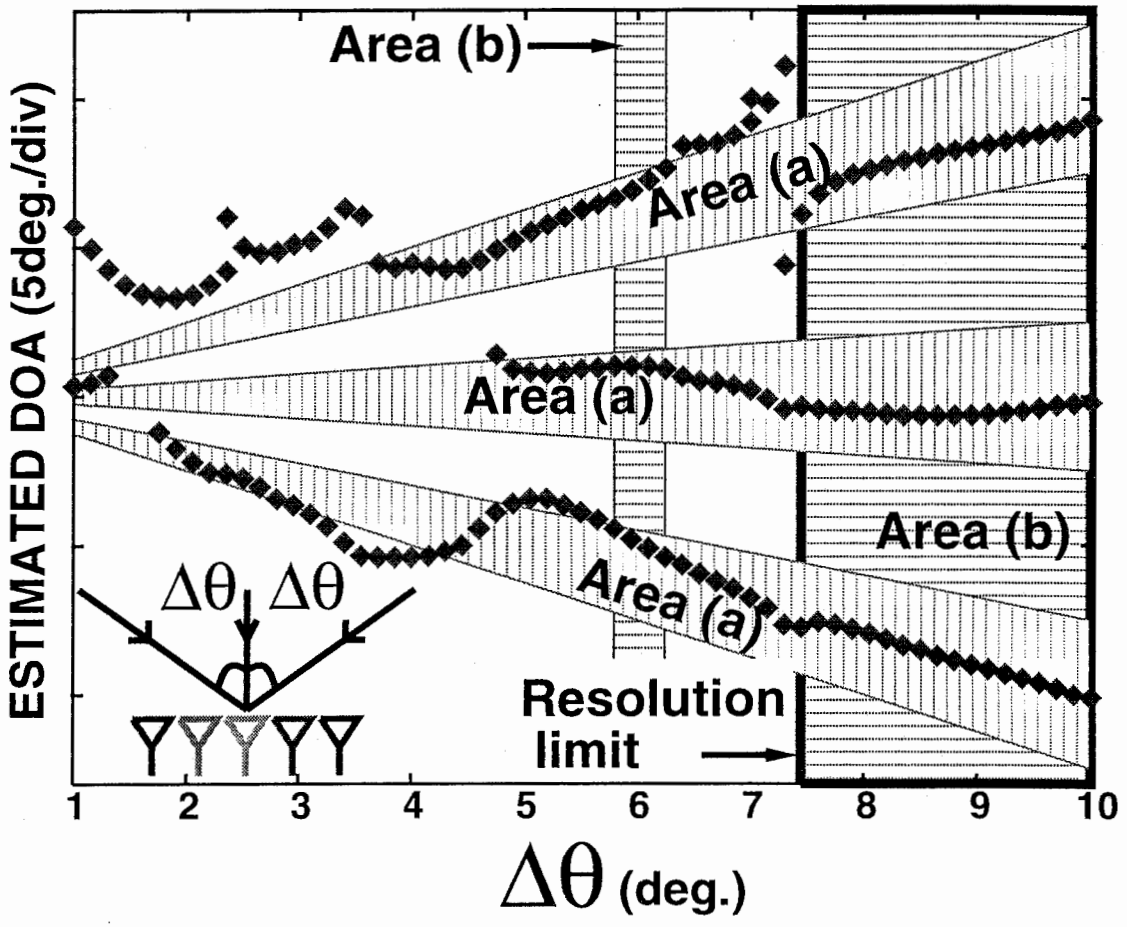

Figure 3: Example of DOA estimation by MUSIC as a definition of the resolution limit when there are three ($P = 3$) incident signals set at intervals of $\Delta\theta$ (0deg. $\leq \Delta\theta \leq$ 10deg.) with additive noise of 0dB. The array system has 32 ($M = 32$) antenna elements. L and K are set as 25 and eight, respectively. $\mathcal{T}_h$ is set as 10^{-3} and the snapshot number H is set to 70.

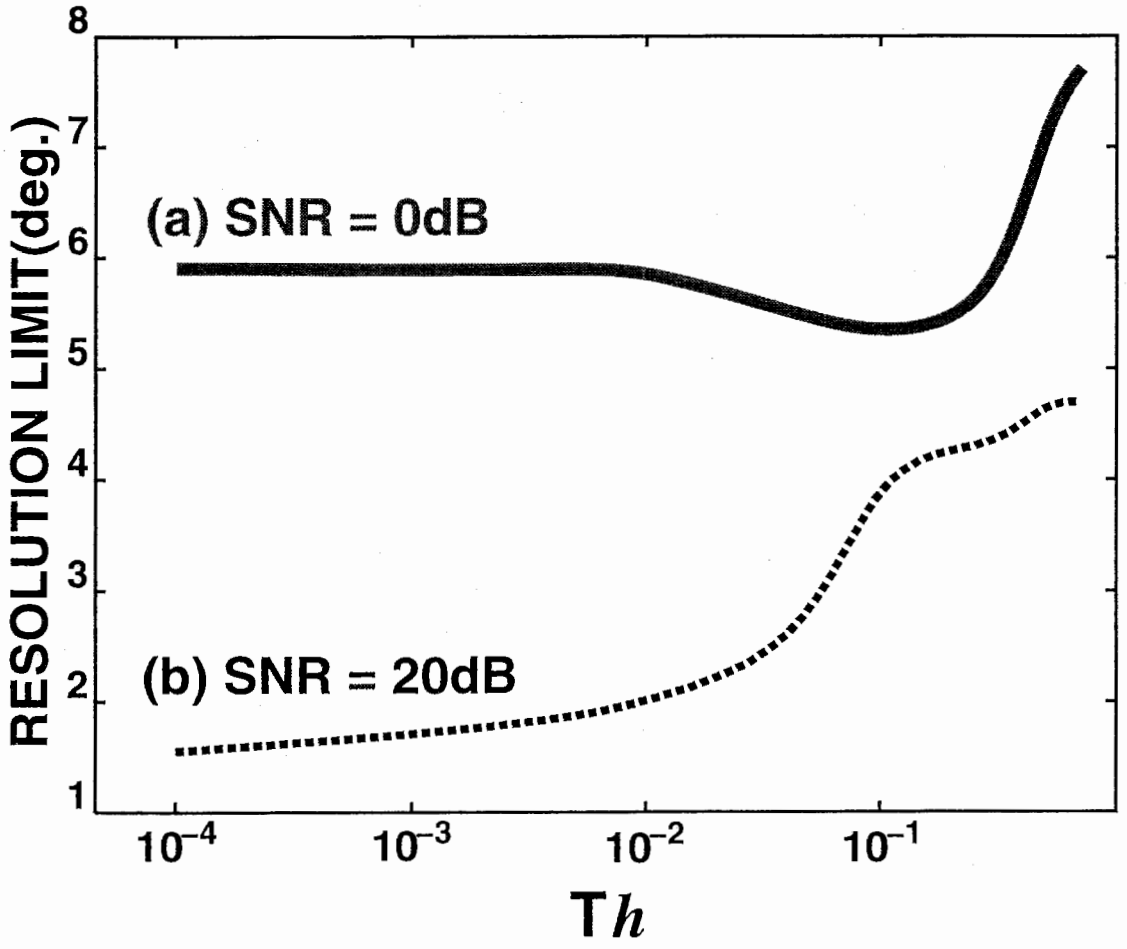

Figure 4: Resolution limit of MUSIC, with $\mathcal{T}_h$ varying from 10^{-4} to 0.7. H and P are set as 70 and 3, respectively.

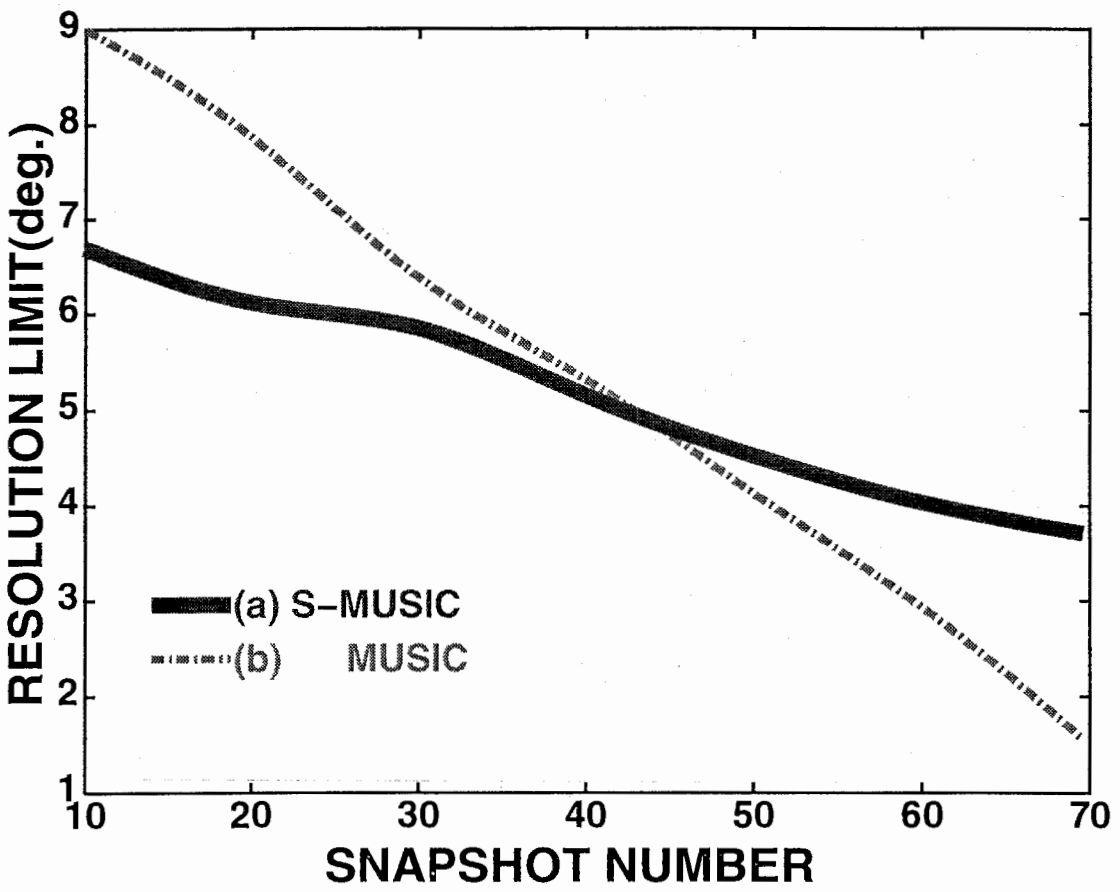

Figure 5: Resolution limits when $\mathcal{T}_h$ in S-MUSIC, and $\mathcal{T}_h$ in MUSIC are set as 0.5 and 10^{-3}, respectively and H ranges from 10 to 70. $\frac{P}{M}$, M, and SNR are $\frac{4}{25}$, 100, and 0dB, respectively.

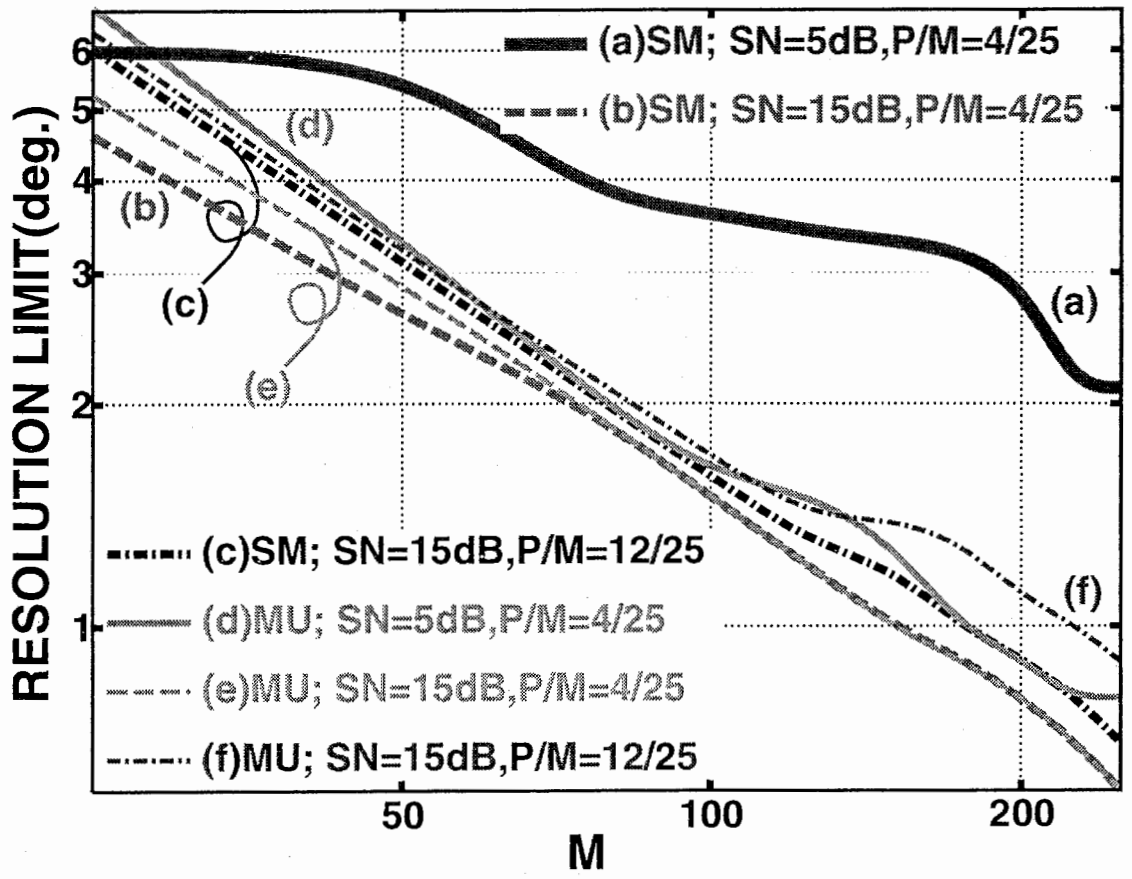

Figure 6: Resolution limits of S-MUSIC and MUSIC when SNR and $\frac{P}{M}$ are fixed and M ranges from 25 to 250. Lines (a), (b), and (c) are the resolution limits of S-MUSIC and lines (d), (e), and (f) are those of MUSIC.

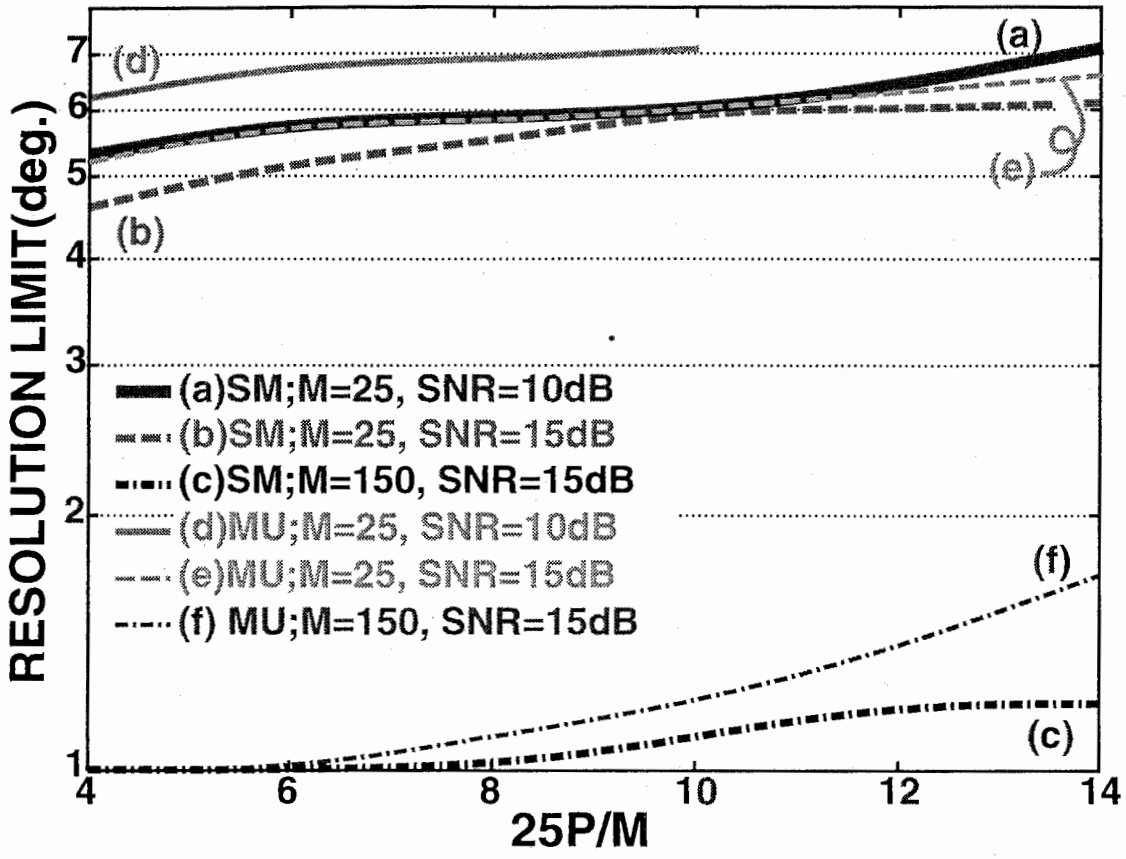

Figure 7: Resolution limits when M and SNR are fixed and $\frac{P}{M}$ ranges from $\frac{4}{25}$ to $\frac{14}{25}$. Lines (a), (b), and (c) are the resolution limits of S-MUSIC and lines (d), (e), and (f) are those of MUSIC.

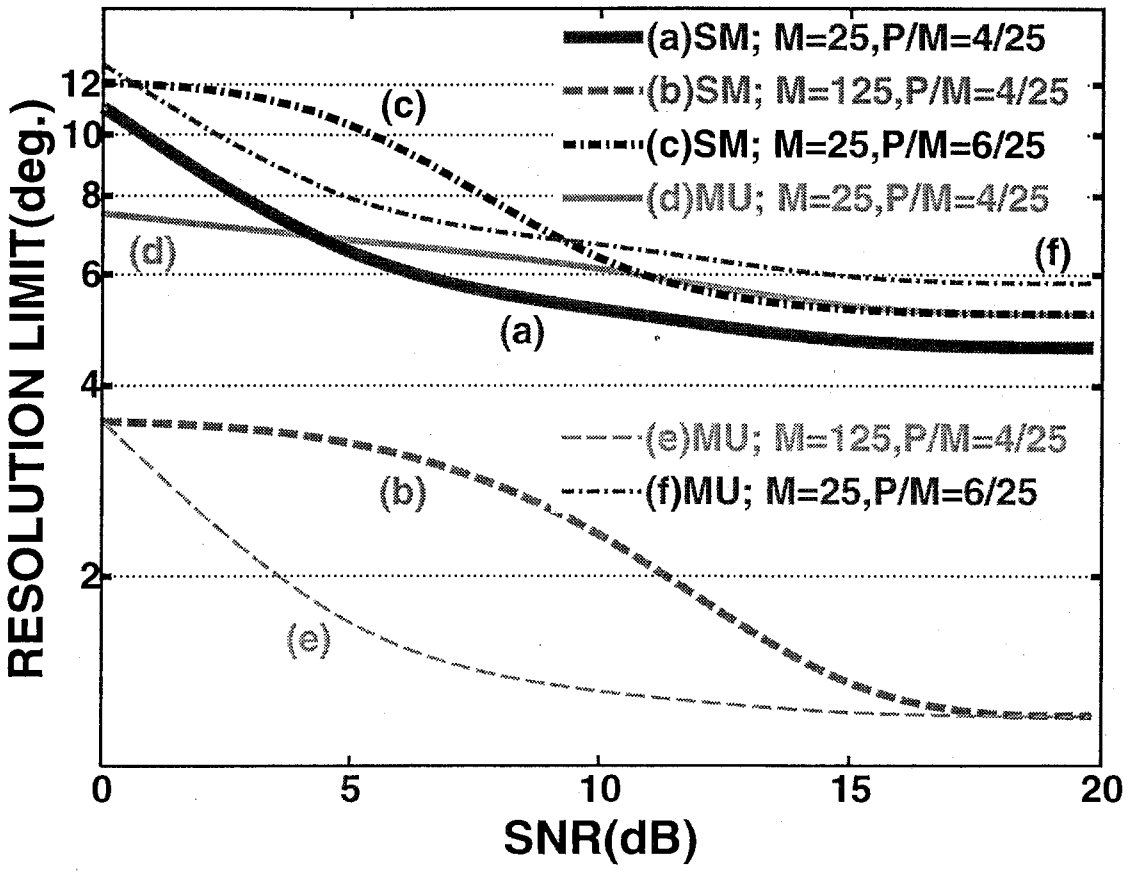

Figure 8: Resolution limit when M and $\frac{P}{M}$ are fixed and SNR ranges from 0dB to 20dB. Lines (a), (b), and (c) are the resolution limits of S-MUSIC and lines (d), (e), and (f) are those of MUSIC.